Available online at www.sciencedirect.com
SCIENCE DIRECT
Journal of Power Sources 154 (2006) 106–114
JOURNAL OF POWER SOURCES
www.elsevier.com/locate/jpowsour

Dual-phase electrolytes for advanced fuel cells

Jiandong Hu [a], Sebastiano Tosto [b,*], Zuoxing Guo [a], Yufeng Wang [c]

[a] *Key Laboratory of Automobile Materials, Ministry of Education, College of Materials Science and Engineering, Microanalysis Centre, Jilin University, Changchun 130025, PR China*
[b] *ENEA Casaccia, via Anguillarese 301, 00060 Rome, Italy*
[c] *Department of Product Configuration (Afd. 3560), Aalborg Industries A/S, P.O. Box 661, Gasvaerksvej 24, 9100 Aalborg, Denmark*

Received 18 October 2004; received in revised form 17 February 2005; accepted 14 March 2005
Available online 6 June 2005

Abstract

Double-phase electrolyte (DPE) consisting of doped CeO_2/NiAl solid phase and NaOH liquid phase was used for fuel cells utilizing $LiNiO_2$ anode and Ag cathode at working temperatures over 450 °C. It was shown that the cells can produce a maximum output power of 716.2 mW cm^{-2} at 590 °C even though utilized with relatively large thickness of electrolyte, from 0.8 to 1.2 mm. Most measurements of open circuit voltage (OCV) range between 1 and 1.2 V; a significantly higher OCV value of 1.254 V was also obtained. Liquid channel conductive mechanism of NaOH in DPE is proposed; both O^{2-} and H^+ concur to conduct the current; the doped CeO_2 transports O^{2-} ions, whereas the molten second phase transports H^+ protons. Moreover, SEM observations and EDS analysis suggest that Na^+ and OH^- also contribute to enhance both OCV and output power of our cells. The addition of NiAl to the doped CeO_2 increases the mechanical strength and the output power of DPE; however the reasons of this latter effect are still to be further investigated. The results show that DPE is a promising electrolyte to manufacture fuel cells with advanced performances.

Keywords: Double-phase electrolyte (DPE); Fuel cell; NiAl; NaOH; Enhanced output power

1. Introduction

The working principles of fuel cells, first reported by Grove [1], enable clean power generators and plants to be engineered in the near future. Some examples of fuel cell power sources have been already set up [2]. Current fuel cells include proton exchange membrane fuel cell (PEMFC), solid oxide fuel cell (SOFC), alkaline fuel cell (AFC), phosphorous acid fuel cell (PAFC) and molten carbonate fuel cell (MCFC). The former two use solid electrolytes, the other ones liquid electrolytes. As concerns the operating conditions, the cells are classified depending on the working temperatures. SOFCs are attractive in particular for power stations and use typically yttrium stabilized zirconia (YSZ) electrolytes at working temperatures of about 1000 °C. If constructed with YSZ film electrolyte, supported with anode, SOFCs allow an operating temperature range of 700–800 °C [3].

Doped CeO_2 is usually utilized as electrolyte of intermediate temperature solid fuel cells (ITSOFC) [4–10], working with oxygen ion and typically operating in a range of temperatures from 400 to 700 °C. On the other hand, inorganic solid compounds such as $CsHSO_2$ [11] (Sr, Ba)CeO_3 [12] and $BaCeO_3$ [13], working as electrolytes with protons, can also make fuel cells operating at lower temperature. Significant results on composite electrolytes consisting of doped CeO_2 with additions of NaOH and salts are reported in [6–8].

In our study, we have realized a new composite electrolyte adding NaOH to an initial mixture of powders of NiAl intermetallic alloy and CeO_2 doped with Gd_2O_3. The addition of NiAl was suggested by the observation that often second metallic phases in doped electrolytes increase the output power [14]. Moreover, the formation of Al_2O_3 film/overlayer on NiAl, reported in [15–17], suggests that NiAl could work in the doped CeO_2 as Al_2O_3 did in PbI_2 [18].

* Corresponding author.
E-mail address: tosto@casaccia.enea.it (S. Tosto).

0378-7753/$ – see front matter © 2005 Elsevier B.V. All rights reserved.
doi:10.1016/j.jpowsour.2005.03.225

It is known that CeO_2 ensures good O^{2-} conduction in ITSOFC, especially, after doping with Gd_2O_3 [19], whereas NaOH has been utilized for AFC electrolytes since the 60s decade [20]; our experimental activity aimed then to realize a new composite electrolyte formed by doped CeO_2 plus NiAl and NaOH and characterized by enhanced conductivity. Characteristic feature of this kind of electrolyte is that it is biphasic solid at room temperature, whereas solid and liquid phases form at working temperature above 400 °C because of melting of NaOH. This new composite electrolyte is referred hereafter as double-phase electrolyte (DPE). The technological interest of our results rests on the fact that the thickness of DPE has no evident influence on the output power, so that film electrolyte materials are unnecessary for good performances. The fuel cells are then easily manufactured and engineered, are robust and can be utilized as stand alone components in a variety of applications.

2. Experimental procedures

The basic constituent of DPEs is the powder of Ce/Gd oxides $Ce_{0.9}Gd_{0.1}O_{1.95}$ (CGO), prepared by solid-state reaction during sintering of CeO_2 (99.96% purity) and Gd_2O_3 (99.5% purity); the size of CeO_2 and Gd_2O_3 powders is in the range 100–400 nm. The $Ce_{0.9}Gd_{0.1}O_{1.95}$ oxide was then mixed with 10.8 wt% of commercial NiAl powder, having size in the range 100–600 nm and fired for 3 h at 900 °C. The NiAl phase has B2 structure with lattice parameter 0.2887 nm and Ni content ranging from 45 to 60% [21]. The mixture was fired in order to form Al_2O_3 film on NiAl by surface oxidation. Subsequently, the resulting mixture was blended with variable amounts of NaOH in order to obtain various NiAl/NaOH compositions; mixtures with weight ratios 100:0 (pure NiAl), 95:5, 92:8, 90:10, 88:12 and 85:15 were the obtained; the result was a three-phase mixture [$Ce_{0.9}Gd_{0.1}O_{1.95}$/NiAl/NaOH]. This latter and the $LiNiO_2$ powder were separately filled into a cylindrical steel die and pressed at 10–20 MPa to form a compacted pellet consisting of two layers. The size of the pellets had diameter of 12 mm, with three final thicknesses of DPE layers equal to 0.8, 1 and 1.2 mm. The effective working area of the pellet was 0.5 cm^2. The DPE side of the pellet was eventually coated with silver glue as cathode to complete the final design of the cell, formed, therefore, by anode of $LiNiO_2$ and cathode of Ag as sketched below:

$$\underset{\text{anode}}{H_2, LiNiO_2} \,/\text{DPE}/\, \underset{\text{cathode}}{Ag, O_2(\text{air})}$$

The cell testing apparatus together with the measurement circuit is given in Fig. 1. The silver glue was pasted on the surface of the holders in contact with the cell pellet to seal the H_2 and air rooms of the device. Anode and cathode were then exposed, respectively, to dry H_2 and air to test the performances of the DPE fuel cells; both gases were allowed to flow with rate of 45 mL min^{-1} at a pressure of about 1.2 atm into

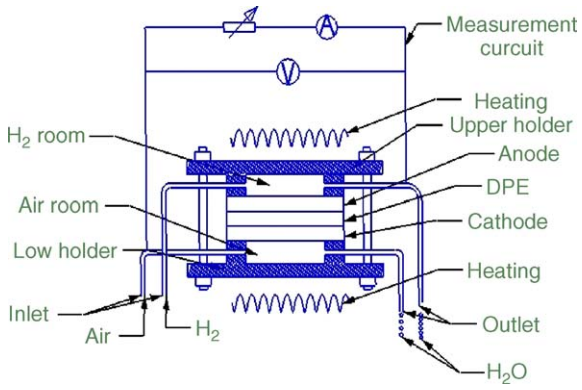

Fig. 1. Scheme of fuel cell.

the respective rooms of the cell and then to come out from the other side of the tube. A series of open circuit voltage (OCV) and voltage/current values were measured properly changing the resistance of the measurement circuit at constant temperature. To this purpose the measurement device was heated in furnace at controlled temperature; then the measurements were repeated at progressively higher temperatures between 400 and 700 °C, thus enabling the cell potential and current to be determined as a function of temperature in a range where usually a peak power is expected. Common copper electricity wires were connected with the tubes to set up measurement circuit. To measure voltage and current, a voltmeter with input resistance of 2000 Ω was employed. SEM observations were then carried out for either new pellets or used pellets to investigate possible changes in materials. Further DPEs were fabricated in order to determine the density with the well-known Archimedes method.

3. Results and discussion

3.1. Possible working principles of DPE

The working principles of DPEs at room temperature and over 400 °C are sketched in Fig. 2a and b, respectively. Since the melting point of NaOH is 318 °C, NaOH and $Ce_{0.9}Gd_{0.1}O_{1.95}$/NiAl form a mechanical solid mixture below 300 °C; as it typically occurs in powder metallurgy, the compacted material is porous, whereas NaOH forms a network of second phase between the grains as shown in Fig. 2a. Small channels are, therefore, likely to be formed through the sintered grains, some of which are also expected long enough to run through the whole thickness of the electrolyte, thus getting in touch with both anode and cathode. When the working temperature overcomes 400 °C, NaOH melts and produces then narrow liquid channels between the grains of $Ce_{0.9}Gd_{0.1}O_{1.95}$, as shown in Fig. 2b; hence, the double-phase electrolyte is formed by solid phase surrounded by channels of liquid phase, whose total amount is equal to the amount of solid NaOH initially added. Fig. 2c shows a SEM micrograph taken from the side surface of DPE of a

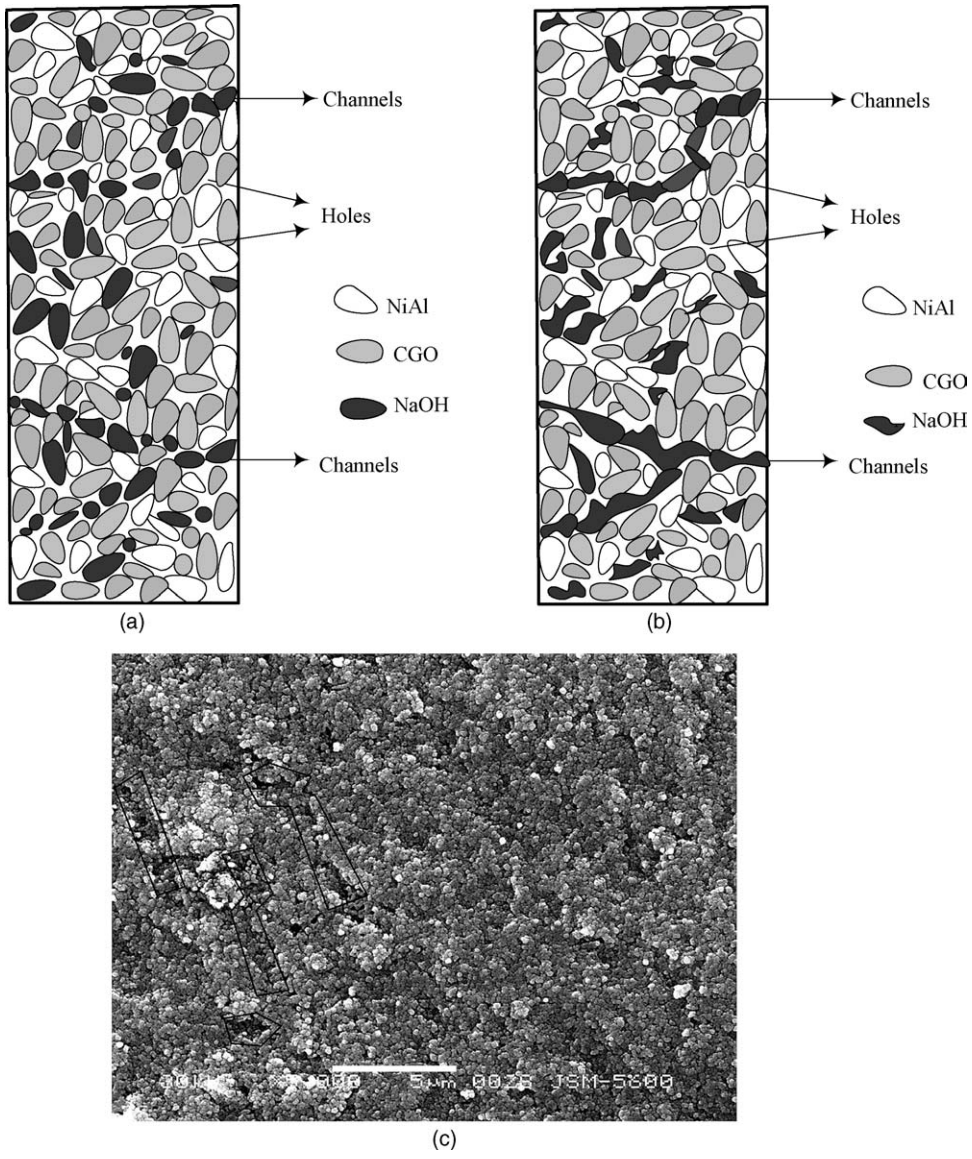

Fig. 2. Cross-section sketch of DPE operating at: room temperature (a) and 400 °C (b); (c) SEM micrograph of the side surface of DPE showing many small holes, marked by squares, which are thought to be the end of channels sketched in (b).

cylinder fuel cell ready for testing; before SEM observation, water was dropped in the cylinder until NaOH was dissolved out, then the sample was heated at 600 °C for 8 h. Several deep small holes and crack-like grooves are visible in figure, some of which are evidenced with polygonal marks. These features may be related to the formation of the channels on the plane of figure and perpendicularly to it, in agreement with the hypothesis sketched in Fig. 2a and b. This conclusion is consistent with the density measurements of DPE, resulting equal to 4.02 g cm^{-3}, i.e. about 56% of the theoretical density 7.22 g cm^{-3} of CeO_2 [19]. This result agrees, in turn, with that reported in literature, according which compacting $(CeO_2)_{0.82}(GdO_{1.5})_{0.18}$ with pressure of 50 MPa yielded an experimental density about 53.5% of the theoretical value [22]. These results suggest that our DPEs contain in fact a lot of pores, some of which can be connected to form channels for H^+ transport, thus supporting the channel conductive mechanism [22]. If so, the doped CeO_2 acts as solid electrolyte, as it does in the usual SOFCs [23], whereas at the same time the liquid channels enable bypass path for transferring H^+. Also, the experimental evidence that water forms both at anode and cathode further supports this hypothesis; H^+ moves along the liquid channels from the anode to the cathode, where it combines with oxygen ions to form water; also, O^{2-} diffuses through the doped CeO_2 by vacancy jumps, as it usually happens in solid electrolytes, to form water with H^+ protons at anode. The formation of water was detected inserting a glass bars into the tubes of gas outlet; in effect, water condensation was observed on the glass bars as long as energy was supplied by the cell. Thus, it is believed that DPE is working through multi-ion conduction mechanisms (MICM) involving both H^+ and O^{2-}. The global fuel

Table 1
Properties of DPE cells containing 12% NaOH, numbered from 1 to 31 and CGO cells, numbers 32 and 33

Cells	OCV (V)	Voltage (V)	Current (mA cm^{-2})	P_{max} (mW cm^{-2})	T_{max} (°C)
1	1.027	0.62	859.35	532.8	630
2	1.149	0.61	888.36	541.9	588
3	1.254	0.68	544.12	370.0	622
4	1.073	0.62	589.84	365.7	664
5	1.062	0.69	638.99	440.9	550
6	1.101	0.60	634.00	380.4	574
7	1.036	0.66	701.52	463.0	660
8	1.162	0.64	675.00	432.0	634
9	1.062	0.64	1119.06	716.2	590
10	0.930	0.65	327.54	212.9	610
11	1.07	0.7	385.71	270.0	589
12	1.004	0.69	678.70	468.3	610
13	1.020	0.71	380.70	270.3	589
14	1.02	0.64	468.91	300.1	635
15	1.038	0.71	631.13	448.1	627
16	0.928	0.64	511.88	327.6	659
17	1.127	0.67	611.04	409.4	632
18	0.999	0.67	415.07	278.1	680
19	1.072	0.63	564.76	355.8	600
20	1.120	0.61	739.02	450.8	630
21	1.02	0.64	359.06	229.8	540
22	1.044	0.70	823.43	576.4	640
23	1.103	0.61	1085.74	662.3	654
24	1.049	0.67	663.73	444.7	590
25	1.091	0.68	408.82	278	580
26	1.07	0.72	519.17	373.8	498
27	1.206	0.65	821.54	534	630
28	1.009	0.63	426.19	268.5	650
29	0.935	0.63	676.03	425.9	644
30	1.066	0.61	757.38	462	661
31	1.004	0.65	500.92	325.6	650
32 (CGO)	0.833	0.5	6.00	3	588
33 (CGO)	0.881	0.4	10.00	4	683

cell reaction, $2H_2 + O_2 = 2H_2O$ + electricity + heat, entails, therefore, water formation assuming that two oxygen atoms approach each other to form non-linear O–H–O transition complex; this transferring mechanism was suggested for H^+ in NaOH in [24]. Significant support to the assumption of the H^+/O^{2-} driven MICM comes also from the electrochemical properties of the cells, reported in the following subsection (Section 3.2).

3.2. Properties of DPE

Table 1 shows the properties of a group of 31 cells fabricated with DPE containing 12% NaOH; the numbers 32 and 33 refer to plain $Ce_{0.9}Gd_{0.1}O_{1.95}$ cells. OCV is the open circuit voltage; the values of current and voltage are used to calculate the maximum output power (P_{max}) at the corresponding working temperatures T_{max}. The average value of P_{max} measured on 31 DPE cells at the average temperature of 615 °C is 406.9 mW cm^{-2}, much higher than the respective values of CGO cells. The highest value of P_{max} of our hydrogen–air cells is 716.2 mW cm^{-2} at 0.639 V and 590 °C, thus, comparable with the value 600 mW cm^{-2} reported in Ref. [7] at 500 °C for the cell NiO + (YDS + 15 wt%NaOH)/YDS + 15 wt%NaOH/lithiated NiO + (YDS + 15 wt%NaOH) and in Ref. [8] at 640 °C for the cell

$$0.4\text{NiO} + 0.4\text{YDS} + 0.2\text{Carbon/YDS} + 5\text{–}30\ \text{wt\%NaOH/La}_{0.6}\text{Sr}_{0.4}\text{Co}_{0.8}\text{Fe}_{0.2}\text{O}_3$$

Most of our OCVs range between 1 and 1.2 V; the maximum measured value is 1.254 V, significantly higher than the other ones. Figs. 3 and 4 are based on the data of Table 1; the former shows that P_{max} of DPE cells decreases at temperatures above 700 °C, the latter evidences the temperature dependence of the voltage V_{pmax} corresponding to P_{max}; all the values are higher than 0.6 V, appropriate for power supply. OCV decreases with increasing temperature. From the data of Table 1 the following simple formula is inferred:

$$V_{pmax} = 0.61\,\text{OCV}$$

The higher OCV, the higher V_{pmax}, which in turn also means that even higher output power can be achieved. The deviation of V_{pmax} with respect to the average value 0.65 V calculated for 31 cells of Table 1 is between +0.07 and −0.05 V.

These performances are considerably better than obtained with usual electrolytes under analogous test conditions. Yet, the stability of output power is not good: typical values of

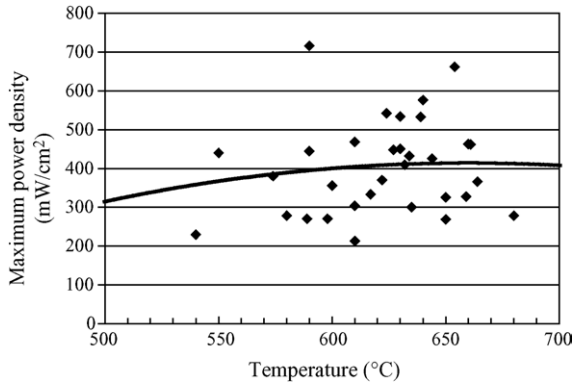

Fig. 3. Relationship between temperature T_{max} and maximum power P_{max} of DPE containing 12 wt% of NaOH.

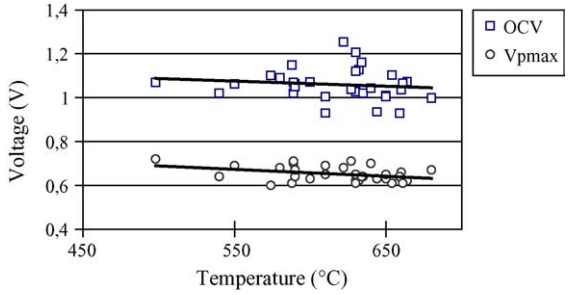

Fig. 4. Relationship between T_{max}, OCV and V_{pmax} of DPE containing 12 wt% of NaOH.

voltage, current and power as a function of working time at constant test temperature show that the output power of a cell with DPE drops from 444.7 to 218.4 mW cm^{-2} after about 4.5 h at 600 °C, see Table 2. This trend might result because of not well-matched anode–DPE–cathode materials or because of possible composition changes of DPE as a function of time occurring at the testing temperatures. The fact that the differences in maximum values of powers are quite large in the group of 31 cells, the dropping to the lowest P_{max} value 212.9 mW cm^{-2} at 610 °C is also thought to result from the above mentioned reason.

Table 2
Electrical performances of a cell made by DPE cell containing 12% NaOH as a function of time

	Δt (min)					
	0	5	20	105	215	275
T_{max} (°C)	598	599	605	610	590	590
Voltage (mV)	654	651	642	691	610	600
Current (mA cm^{-2})	680.0	678.2	667.4	416.0	368.0	364.0
Power (mW cm^{-2})	444.7	441.5	428.5	287.5	224.5	218.4

The electric performances are summarized in the Tables 3 and 4 and in Figs. 3–7. Table 3 shows a series of powers for a typical DPE cell containing 12% NaOH at temperatures ranging from 563 to 698 °C. R_∞ refers to the situation of open circuit, so that V is actually the OCV value; R_i are the total resistances, progressively decreasing from R_1 to R_6, corresponding to the measured values of voltage V and current I of an electrical circuit with variable external load to which were connected the cells. It appears that, for any given total resistance, the output power increases with the operating temperature until maximum value at 654 °C, beyond which it decreases. These data, together with analogous measurements carried out on plain CGO and composite CGO/NiAl electrolyte cells not reported in Table 3 for brevity, were used to draw Fig. 5a–c; these figures compare the relationship

Table 3
Voltages V (volt) and currents I (mA cm^{-2}) of DPE cells containing 12% NaOH measured at various temperatures

T (°C)	Voltage and current	R_∞ (OCV)	R_1	R_2	R_3	R_4	R_5	R_6
563	V	1.103	0.979	0.921	0.693	0.600	0.481	0.364
	I	0	0.011	0.027	0.127	0.180	0.251	0.319
570	V	0.992	0.975	0.946	0.757	0.653	0.531	0.409
	I	0	0.011	0.027	0.136	0.195	0.274	0.355
585	V	0.956	0.940	0.914	0.764	0.672	0.561	0.453
	I	0	0.010	0.027	0.137	0.220	0.291	0.398
626	V	0.956	0.950	0.935	0.820	0.747	0.642	0.525
	I	0	0.010	0.027	0.149	0.224	0.335	0.458
637	V	0.977	0.970	0.959	0.856	0.785	0.689	0.570
	I	0	0.011	0.028	0.154	0.234	0.356	0.497
646	V	0.987	0.979	0,966	0.870	0.800	0.602	
	I	0	0.011	0.028	0.158	0.240	0,525	
654	V	0.980	0.973	0.959	0.873	0.810	0.613	
	I	0	0.011	0.028	0.158	0.243	0.540	
687	V	0.956	0.948	0.936	0.855	0.798	0.610	
	I	0	0.027	0.027	0.155	0.239	0.537	
698	V	0.922	0.920	0.911	0.836	0.782	0.695	0.585
	I	0	0.010	0.260	0.152	0.235	0.364	0.514

The first column of data reports the open circuit voltage of the cells, $R = \infty$.

Table 4
Comparison between the maximum power P_{max} of our [$LiNiO_2$/DPE/Ag] cells containing contain 12% NaOH and various SOFCs cells reported in literature

Reference	Electrolyte	Thickness of electrolyte (mm)	Power density (mW cm^{-2})//voltage (V)	Temperature (°C)
[25]	$Ce_{0.8}Gd_{0.2}O_{1.9}$	0.03	140//0.7	500
[26]	Y_2O_3 doped with ceria + zirconia	0.005–0.0095	250	600
[27]	$BaTh_{0.9}Gd_{0.1}O_3$		200//0.7	550
[28]	$La_{0.9}Sr_{0.1}Ga_{0.8}Mg_{0.2}O_{2.85}$	0.189	500//0.7	600–800
[29]	$Ce_{0.8}Gd_{0.2}O_{1.9}$	0.1–0.25	150//0.7	603
DPE	$Ce_{0.9}Gd_{0.1}O_{1.95}$/NiAl/NaOH	0.8	716.2//0.639 (maximum)	590

Table also reports the test temperatures and the thickness of the electrolytes.

between voltage and current density of DPE, CGO + NiAl and plain CGO cells, respectively, operating with the same anode and cathode. The results show that the DPE cells have the best performances, whereas the CGO/NiAl cells have higher power than the plain CGO cells. Although the experimental evidence shows that the addition of NiAl to the doped CeO_2 increases the mechanical strength and the output power of both CGO and DPE cells, the microstructural mechanisms enabling these effects are still to be fully understood.

The results of Table 4 emphasize in particular that the typical thickness of the usual electrolyte materials is of the order of 0.005–0.25 mm, whereas that of our DPE has much larger values, about 0.8–1.2 mm. In general, the thickness significantly increases the internal resistance of the electrolyte, thus, decreasing the global efficiency of the cell; in the present case, however, it appears from Fig. 6 that the thickness does not affect significantly the electrical performances. On the one side, the fact that DPE still keeps good conductivity

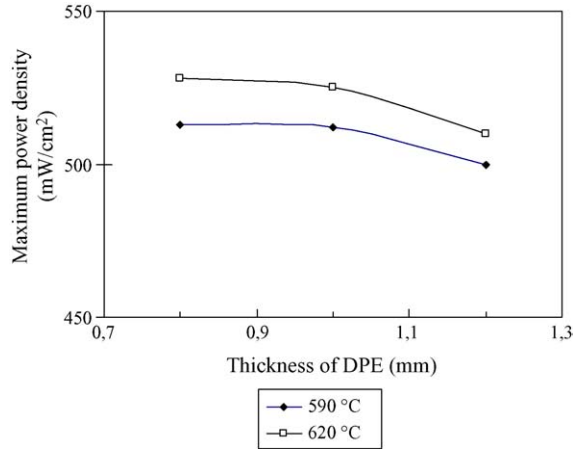

Fig. 6. Relationship between output power and thickness of DPE cells containing 12 wt% of NaOH.

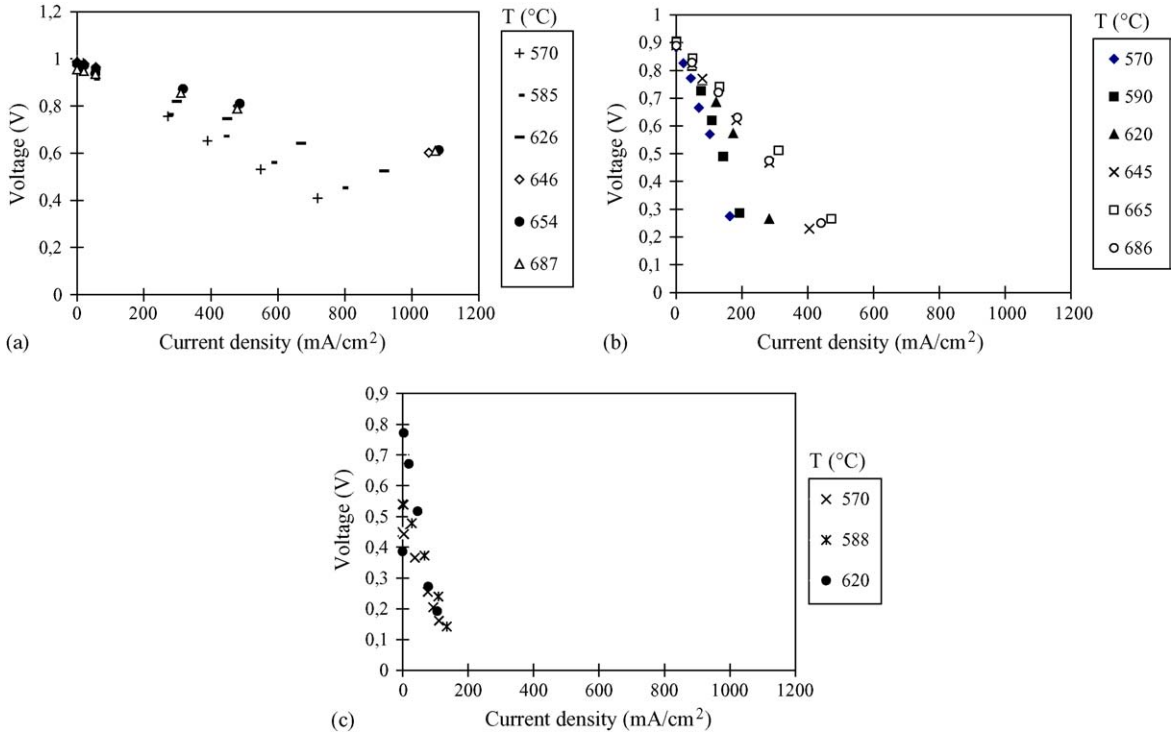

Fig. 5. (a) Voltage vs. current density of cells with DPE containing 12 wt% of NaOH; (b) voltage vs. current density of cells with CGO + 10.8 wt% NiAl electrolyte; (c) voltage vs. current density of cells with plain CGO electrolyte.

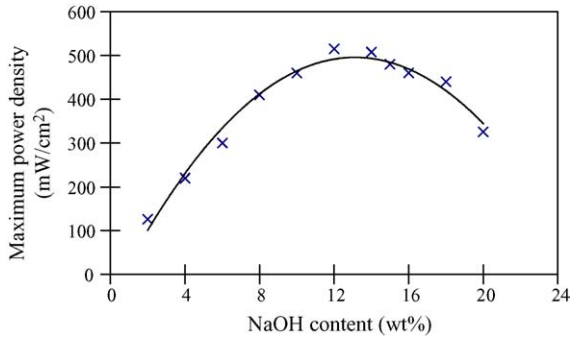

Fig. 7. Output power of DPE cells with variable NaOH content.

even with such large thickness can be explained by assuming that the liquid channel are actually the dominant conducting phase, thus, confirming that the double-phase electrolyte has H^+/O^{2-} mixed-ionic conducting system; the main way for H^+ is the convection through the liquid phase channels, whereas for O^{2-} is the diffusion through the bulk $Ce_{0.9}Gd_{0.1}O_{1.95}$, as usual. On the other side, the high-power density achieved demonstrates that thin electrolytes are not necessary, whereas the cell working temperature could be in principle even lower than 400 °C; for this reason, the process for DPE production is in principle simple, our fuel cells are inexpensive, robust and easy to be fabricated. The electrical performances are optimized with about 12 wt% of liquid phase, as it appears in the plot of Fig. 7 showing the maximum output power as a function of the NaOH content. The experimental results show then that DPE may be a good candidate for advanced fuel cell devices operating at low temperature. It is known that the grain boundary conductivity is rather lower than that of bulk crystal of CGO, because of some impurities like SiO_2 formed on the grain boundary. In our study, NaOH around CGO grains according to the scheme of Fig. 2a and b seems instead effective in increasing the conductivity. To discuss this point, the next subsection (Section 3.3) reports the results of microstructural characterization by scanning electron microscopy (SEM) observations and X-ray energy dispersive microanalysis (EDM).

3.3. Microstructural investigation of DPEs

SEM observations have been carried out on pellets after testing at several temperatures for about 6 h. Cracks are observed on some $LiNiO_2$ anode layers, see Fig. 8, whereas the interface between anode and DPE was not hardly damaged during the test. The silver cathode layer was damaged by NaOH corrosion, as it appears in Fig. 9, leading to decreased output power of DPE cells.

EDM was carried out on several zones of the fracture surface of DPEs utilizing local X-ray emission of Ce, Ga, O, Na, Ni and Al. The distribution of Ga overlaps that of Ce; the results for the other elements are shown in Fig. 10a–f. Some precipitates are observed, some of which were, in turn, analysed. Two precipitates marked in Fig. 10a (secondary electron

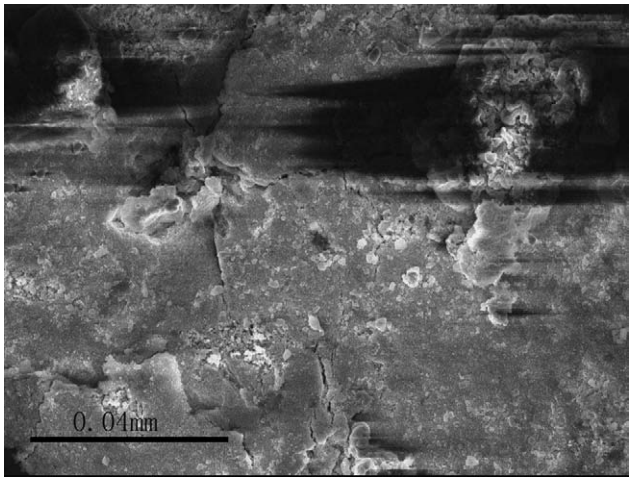

Fig. 8. SEM micrograph showing some cracks in the anode; the cell operated at 600 °C for 1 h.

image) are identified as NaOH; Fig. 10c shows that the Na distribution is inhomogeneous in the area examined. However some Na-rich zones do not show appreciable presence of oxygen, as it appears in Fig. 10b. It is thought, therefore, that these precipitates are sodium resulting from the decomposition of NaOH according to the reaction $NaOH \rightarrow Na^+ + OH^-$; therefore, Na^+ and OH^- may also play themselves some role in the enhanced output power of DPE cells, since it is likely that also Na^+ and OH^- might contribute to the total electrical conduction inside the cell, although such a mechanism is still to be investigated. In any case, also the presence of Na^+ and the high OCV value 1.254 V support significantly the hypothesis of MICM.

In Fig. 10e are visible two precipitates located within the channels and remained there even after that NaOH was removed from the channels by dissolution in water. Three other particles marked with "NiAl" in Fig. 10a are identified by the Ni and Al emissions as NiAl particles in the following Fig. 10d and f. It is also interesting to note from Fig. 10b that these three particles are oxygen-rich; it demonstrates, there-

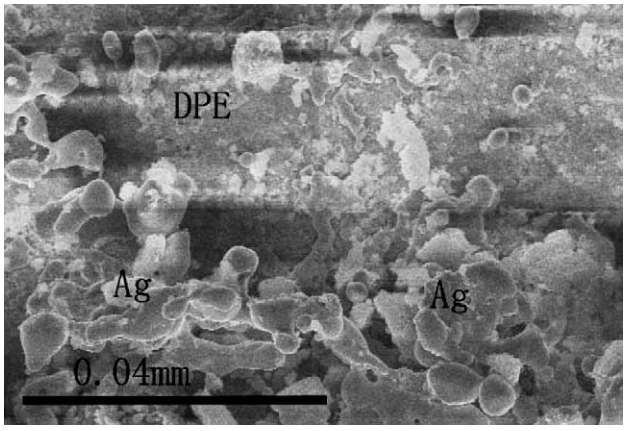

Fig. 9. SEM micrograph showing the damaged silver cathode layer; the cell operated at 600 °C for 1 h.

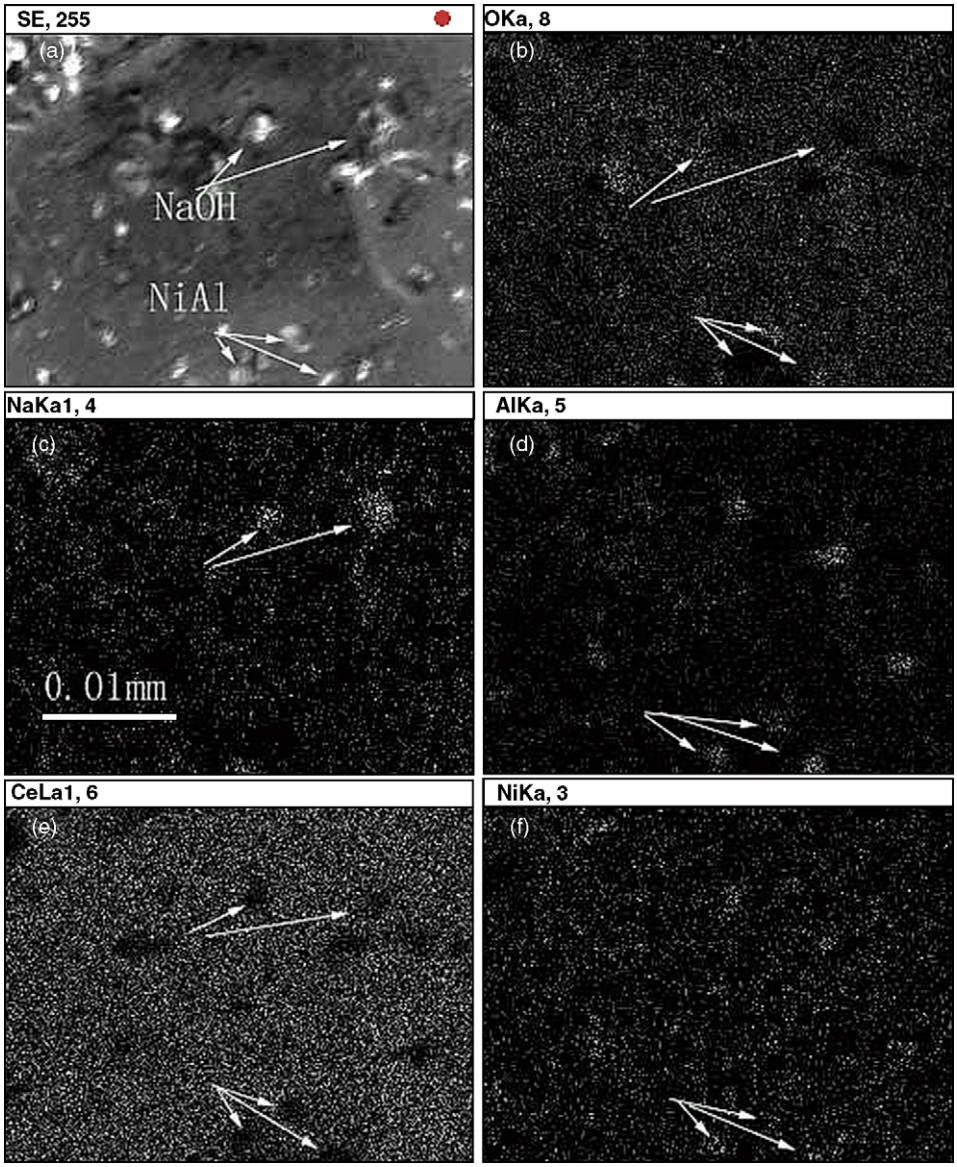

Fig. 10. Element analysis results for a DPE cell containing 12% NaOH; the cell operated at 600 °C for 1 h: secondary electron image (a); O image (b); Na image (c); Al image (d); Ce image (e); Ni image (f); figure shows some NaOH particles, some oxygen-free white precipitates containing Na and three oxygen-, Ni- and Al-rich particles, marked with "NiAl".

fore, that, as expected, a thin oxide film was formed at the surface of the NiAl phase. AFC made by KOH showed better electric performances than NaOH [20]; thus, similar or better performances can be expected using in our cells KOH instead of NaOH.

4. Conclusion

Doped CeO_2 and NaOH enable double-phase electrolytes to be fabricated; the solid mixture at room temperature turns into liquid/solid two-phase system at temperatures above 400 °C. The output power of the cell does not depend appreciably on the thickness of DPE because of its low internal resistance. Both H^+ and O^{2-} are thought to contribute to the output power. The transport bypass for H^+ is due to liquid NaOH. DPE works according to H^+/O^{2-} driven MICM principle; however, the decomposition of NaOH evidenced by EDS analysis and SEM observation suggests that the good conductivity of DPE cells might be related also to Na^+ and OH^- transport in liquid phase. The optimized NaOH composition for DPE is 12 wt%; hence, the partial decomposition of NaOH could be related to the power drop during the test measurements. The maximum output power of fuel cell constructed with $LiNiO_2$ anode and Ag cathode fed with hydrogen can produce at 590 °C power up to 716.2 mW cm^{-2} at 0.639 V. Most values of OCV range from 1 to 1.2 V. The maximum OCV recorded was 1.254 V, significantly higher than the usual values reported in literature. DPEs show significant features of high efficiency and low manufacturing

cost. The next task of our experimental activity is to improve the stability of DPE cells by looking for available cathode and anode that fit better with our DPE and by keeping constant the NaOH content during the tests. The effects of addition of NiAl into the doped CeO_2 must be further investigated in detail, in particular as concerns the formation of oxide films.

References

[1] W.R. Grove, Philos. Magn. 14 (1839) 127.
[2] M. Godlickemeier, L.J. Gauckler, J. Electrochem. Soc. 145 (1998) 414.
[3] S. de Souza, S.J. Visco, L.C. DeJonghe, Solid State Ionics 98 (1997) 57.
[4] C. Xia, M. Liu, Solid State Ionics 144 (2001) 249.
[5] B.C.H. Steele, Solid State Ionics 129 (2000) 95.
[6] B. Zhu, J. Power Sources 93 (2001) 82.
[7] B. Zhu, X. Liu, Peng Zhou, J. Mater. Sci. Lett. 20 (2001) 591.
[8] B. Zhu, J. Power Sources 114 (2003) 1.
[9] K. Choy, W. Bai, S. Charojrochkul, B.C.H. Steele, J. Power Sources 71 (1998) 361.
[10] R. Doshi, L. Von Richards, J.D. Carter, X. Wang, M. Krumpelt, J. Electrochem. Soc. 146 (1999) 1273.
[11] S.M. Halle, D.A. Boysen, C.R. Chisholm, R.B. Merte, Nature 410 (2001) 910.
[12] H. Iwahara, T. Esaka, H. Uchida, Solid State Ionics 284 (1981) 359.
[13] M. Koyama, C.-J. Wen, K Yamada, J. Electrochem. Soc. 147 (2000) 87.
[14] S.W. Tao, Q.Y. Wu, D.K. Peng, G.Y. Meng, J. Appl. Electrochem. 30 (2000) 153.
[15] W. Zhang, J.R. Smith, A.G. Evans, Acta Mater. 50 (2002) 3803.
[16] D. Padmavardhani, A. Gomez, R. Abbaschian, Itermetallics 6 (1998) 229.
[17] A. Stierle, Zeitschrift Fur Metallkunde 93 (2002) 833.
[18] B. Kumar, K. Shahi, J. Mater. Sci. 30 (1995) 4407.
[19] M. Mogensen, N. Sammes, G.A. Tompsett, Solid State Ionics 129 (2000) 63.
[20] F.T. Bacon, Electrochim. Acta 14 (1969) 569.
[21] R.D. Noebe, R.R. Bowman, M.V. Nathal, Int. Mater. Rev. 389 (1993) 193.
[22] I. Riess, D. Braunshtein, D.S. Tannhauser, J. Am. Ceram. Soc. 64 (1981) 479.
[23] O. Yamamoto, Electrochim. Acta 45 (2000) 2423.
[24] B.S. El'kin, Solid State Ionics 37 (1990) 139.
[25] J.K. Kliner, R.J. Brook, Solid State Ionics 6 (1982) 237.
[26] T. Tsai, S.A. Barnet, in: U. Stimming, S.C. Singhal, H. Tagawa, W. Lehnert (Eds.), Proceedings of the Fifth International Symposium on Solid Oxide Fuel Cells, 1997, p. 274.
[27] R. Cook, J.J. Qsborne, J.H. White, R.G. MacDuff, A.F. Sammells, J. Electrochem. Soc. 129 (1992) 19.
[28] T. Ishihara, T. Shibayma, M. Honda, H. Furutani, Y. Takita, Fuel Cell Seminar, Palm Spring, USA, 1998, p. 104.
[29] F.P.F. van Berkel, G.M. Christie, F.H. van Heuveln, J.P.F. Huijsmans, in: M. Dokiya, O. Yamamoto, H. Tagawa, S.C. Singhal (Eds.), Proceedings of Fourth International Symposium on Solid State Fuel Cells, Hagoya, Japan, Electrochemical Society, NJ, USA, 1995, p. 1062.